

# A MODULAR APPROACH TO THE KORBA AQUIFER SEAWATER INTRUSION STUDY, 2, SIMULATION, DATA MANIPULATION, AND VISUALIZATION FOR THE 3-D MODEL

G. Lecca, C. Paniconi, F. Bettio, L. Muscas, and E. Leonardi  
*Environment Group*  
*Centro di Ricerca, Sviluppo e Studi Superiori in Sardegna (CRS4),*  
*Cagliari, Italy*

I. Khlaifi and J. Tarhouni  
*Département de Génie Rural, Eaux et Forêts*  
*Institut National Agronomique de Tunisie (INAT),*  
*Tunis, Tunisia*

## ABSTRACT

Seawater intrusion is an important environmental problem in the coastal aquifers of many Mediterranean countries. In the 438 km<sup>2</sup> Korba aquifer of eastern Tunisia, a large increase in the number of pumping wells for irrigation purposes since the 1960s has resulted in significant lowering of water table levels in several observation piezometers, and in a consequent deterioration of water quality. Due to the important agricultural uses of the Korba plain, several remediation scenarios are being considered for this region, including artificial recharge of the aquifer and construction of small reservoirs to serve as an alternative source of irrigation water. In order to investigate the impact of these measures on aquifer water quality, a modeling study supported by a geographic information system (GIS) and a database management system (DBMS) is being developed. The 3-D finite element model considers coupled density-dependent variably saturated flow and miscible transport. Calibration results and simulations that examine the interplay between recharge and pumping and its effect on the saline water distribution in the subsurface and the unsaturated zone are discussed. Other simulations are used to investigate the location and extent of the window or seepage face controlling freshwater discharge into the sea. Model output data is post-processed to extract the selected time and/or space slices without extensive reformatting to produce 3-D graphical display and animation sequences. Data and model are organized to give the user the ability to increase the understanding of the pollution mechanism and to assess its evolution in the presence of remediation steps.

## INTRODUCTION

In the last twenty years, saltwater intrusion in coastal aquifers has become an important environmental problem worldwide. The problem is particularly serious in the southern part of the Mediterranean basin, where water demand is rapidly increasing with population and water resources are limited.

The Korba aquifer is a part of the western coastal aquifer of the Cap Bon area, which extends from the city of Ras Maamoura in the south to the city of Kelibia in the North, and is bounded by the Mediterranean Sea in the east and the Djebel Abderrahman anticline in the west (see Figure 1). The phreatic alluvial aquifer is 438 km<sup>2</sup> in area and consists of two important formations: a Pliocene sandstone whose

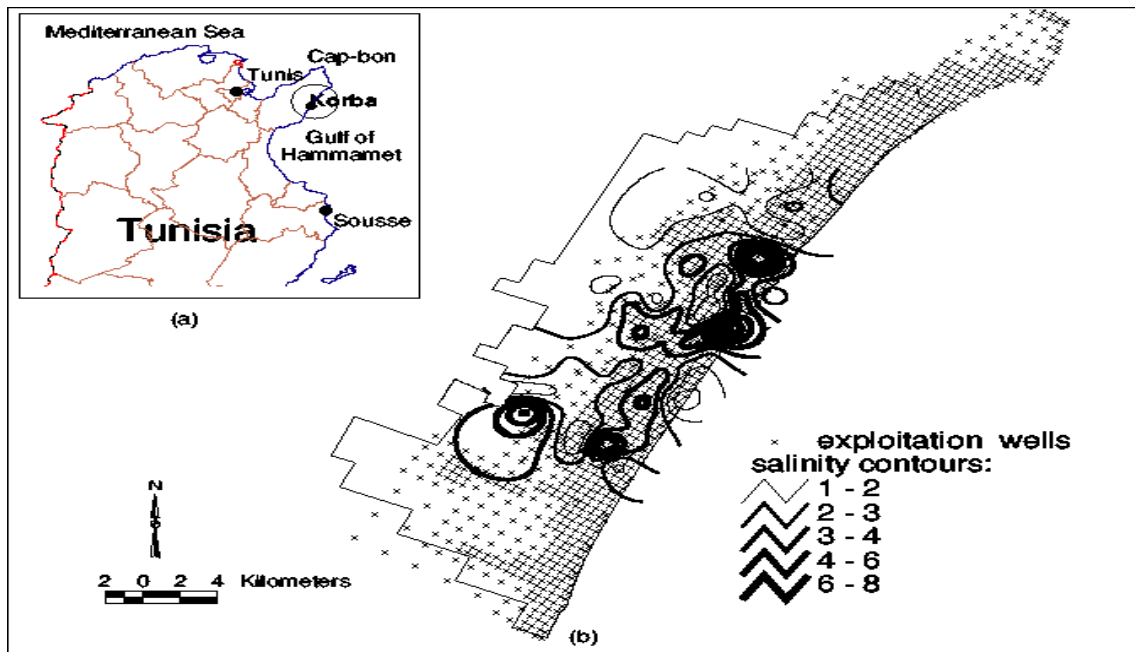


Figure 1. a) Geographic location of the Korba coastal aquifer; b) exploitation map and salinity contours [g/l] from 1996 measurements.

stratigraphic series correspond to an alternation of sandstone and marl, and a Quaternary alluvium containing detrital sediment (sand, gravel, silt) with thin clay lenses. The aquifer depth is in reality highly variable, ranging from 150 m in the south to 30 m in the north, and decreasing from east to west to nearly vanish at the Djebel Abderahman anticline. Recharge of this aquifer is mainly from infiltration from natural replenishment at an average rate of 32 mm/year (Ennabli, 1977), or about 7% of the mean annual rainfall (460 mm).

In the Korba plain the consequence of saltwater intrusion is a decrease in overall irrigated areas, with subsequent production losses, damage to ecosystems, and migration of local populations. In this region land-use changes and irrigation schemes need to be designed and managed so as to minimize the risk of saltwater encroachment. Moreover, remediation measures need to be considered in order to limit the advancing seawater front, including artificial recharge of the aquifer and construction of small reservoirs to serve as an alternative source of irrigation water. In this study, the response of the Korba phreatic aquifer

to selected remediation scenarios is analyzed via a three-dimensional model that handles density-dependent variably saturated flow and dispersive transport.

The model can also treat temporally and spatially variable boundary conditions (rainfall/evaporation, irrigation, pumping) and physical parameters (material, solute, and hydraulic characteristics).

## MATHEMATICAL MODEL

Analyses of saltwater intrusion, assuming that mixing occurs at the transition zone between seawater and freshwater because of hydrodynamic dispersion, requires the solution of two partial differential equations representing the mass conservation principle for the variable-density fluid (flow equation) and for the dissolved solute (transport equation).

The mathematical model of density-dependent flow and transport in groundwater is expressed here in terms of an equivalent freshwater head  $h = \psi + z$ , where  $\psi = p / \rho_o g$  is the equivalent freshwater pressure head,  $p$  is the pressure,  $\rho_o$  is the freshwater

density,  $g$  is the acceleration of gravity, and  $z$  is the vertical coordinate directed upward (Frind, 1982). The density  $\rho$  of the saltwater solution is written in terms of the reference density  $\rho_o$  and the normalized salt concentration  $c$  as  $\rho = \rho_o(1 + \varepsilon c)$ , where  $\varepsilon = (\rho_s - \rho_o) / \rho_o \ll 1$  is the density difference ratio and  $\rho_s$  is the solution density at the maximum normalized concentration  $c = 1$  (density of seawater). The dynamic viscosity  $\mu$  of the saltwater mixture can be considered constant and equal to the viscosity of freshwater within the density range of 1000-1030 g/l typically involved in saltwater intrusion processes. With these definitions, the coupled system of variably saturated flow and miscible salt transport equations is (Gambolati *et al.*, 1998):

$$\sigma \frac{\partial \psi}{\partial t} = -\nabla \cdot v - n S_w \varepsilon \frac{\partial c}{\partial t} + \frac{\rho}{\rho_o} q \quad (1)$$

$$n \frac{\partial S_w c}{\partial t} = \nabla \cdot (D \nabla c) - \nabla \cdot (c v) + q c^* + f \quad (2)$$

with the Darcy velocity vector given by  $v = -K \cdot (\nabla \psi + (1 + \varepsilon c) \nabla z)$ . In the above equations  $K = K_s(1 + \varepsilon c) k_r$  is the hydraulic conductivity tensor, with  $K_s$  the saturated hydraulic conductivity tensor at the reference density and  $k_r(\psi)$  the relative conductivity;  $n$  is the porosity;  $S_w(\psi)$  is the water saturation;

$\sigma(\psi, c) = (1 + \varepsilon c)(S_w S_s + n \frac{dS_w}{d\psi})$  is the general

storage term, with  $S_s$  the specific storage;  $t$  is time;  $q$  is the injected (positive)/extracted (negative) volumetric flow rate;  $c^*$  is the normalized concentration of salt in the injected/extracted fluid;  $f$  is the volumetric rate of injected/extracted solute that does not affect the velocity field; and

$$D = n S_w \tilde{D} = \alpha_T |\mathbf{v}| \delta_{ij} + (\alpha_L - \alpha_T) \frac{v_i v_j}{|\mathbf{v}|} + n S_w D_0 \tau \delta_{ij}$$

is the dispersion tensor, with  $i, j = x, y, z$  and  $\tilde{D}$  defined as in Bear (1979),  $\alpha_L$  and  $\alpha_T$  the longitudinal and transverse dispersivity coefficients,

$$|\mathbf{v}| = \sqrt{v_x^2 + v_y^2 + v_z^2}, \quad \delta_{ij} \text{ the Kronecker delta, } D_0$$

the molecular diffusion coefficient, and  $\tau$  the tortuosity ( $\tau = 1$  is assumed here).

Initial conditions and Dirichlet, Neumann, or Cauchy boundary conditions are added to complete the mathematical formulation of the flow and transport problem expressed in (1) and (2). The nonlinear pressure head dependencies in the general storage and relative hydraulic conductivity terms are expressed through semi-empirical constitutive relationships.

The numerical model is a standard finite element Galerkin scheme, with tetrahedral elements and linear basis functions, and weighted finite differences are used for the discretization of the time derivatives. The system of nonlinear algebraic equations arising from the discretization is solved by an iterative scheme using either the Picard or Newton methods (Putti and Paniconi, 1995).

## DATA MANIPULATION AND VISUALIZATION

The model input and output data have been organized in relational database tables and views. The RDBMS (relational database management system) used to store, update, manipulate, and analyze the data is Oracle 7. Tables and views are updated for each simulation with new data that can be processed by means of proper queries. Oracle and the visualization module have been interfaced by means of an SQL preprocessor for extracting and formatting Oracle data into the appropriate visualization data format.

The model output is then post-processed using AVS (Application Visualization System), a modular visualization environment (MVE) for scientific computation. All the visualizations were generated on an SGI Indigo2 computer. From the end-user point of view, MVE are extremely versatile and flexible. In many cases, setting up a personalized rendering of even complex data simply requires setting up links to pre-existing "modules" within a "data flow" network.

During the computer simulations, the model output is stored in the database and reformatted in the appropriate unstructured cell data (UCD) format, at se-

lected temporal instants, for visualization purposes. The UCD data structure contains the geometrical and topological information and the spatial distributions of some scalar and vector fields such as pressure, concentration and Darcy velocities. From the 3-D dataset we can extract, using an AVS module, the isosurface of zero pressure head (water table) and plot on it both the labeled isolines of surface node elevation and the relative salt concentration contour.

## MODEL APPLICATION AND RESULTS

**Model setup.** The finite element surface mesh used for the numerical simulation of the Korba aquifer contains 1,643 nodes and 2,917 Delauney triangles and follows the digital elevation model of the Korba plain with elevations above sea level (a.s.l.) in the range 0 to 160 m (Khlaifi *et al.*, 1997; Lecca *et al.*, 1998). The same 2-D grid was adopted to cover the aquifer bottom having depths, with reference to the topographic surface, in the range 24 to 150 m. The 3-D grid contains 7 layers of varying depth for a total of 11,501 nodes and 52,506 tetrahedra.

In accordance with the geology of the Korba plain, 3 material subregions have been defined with the corresponding saturated conductivities given in Table 1. The aquifer is assumed isotropic and homogeneous within each subregion.

**Table 1. Saturated conductivities ( $\times 10^{-6}$  m/s)**

Layer	Pliocene formations		Quaternary alluvia
	Sandstone	sand of Sommaa	
1	4.025	2.025	4.025
2÷7	8.025	2.025	8.025

For the entire aquifer the other material and solute properties for the simulations are set to the following values:  $n = 0.25$ ,  $S_s = 0.0012 \text{ m}^{-1}$ ,  $\varepsilon = 0.025$ ,  $\alpha_L = 170 \text{ m}$ ,  $\alpha_T = 7 \text{ m}$ ,  $D_o = 0 \text{ m}^2/\text{s}$ .

**Boundary conditions.** The southern, western, and northern boundaries and the aquifer bottom are treated as impermeable to flow and not allowing mass dispersive flux ( $\partial c / \partial n = 0$ ). On the eastern (coastal) boundary, the flow equation is

fixed real head  $h^* = (p / \rho_O g) + z = k$ , which, expressed in terms of equivalent freshwater head, is  $h = k + (k - z)\varepsilon$ . For the transport equation a zero dispersive flux is imposed over a window of variable depth  $w$  ( $w < 30 \text{ m}$ ) and a prescribed seawater concentration ( $c = 1$ ) is imposed below  $w$ .

Along the rivers Dirichlet boundary conditions are imposed as constant in time freshwater heads equal to the corresponding river bed elevation. The effect of this condition, which implies that the water table lies on the topographic surface, needs to be evaluated.

The Neumann condition of zero dispersive flux along the upper portion of the coastal boundary allows the lighter freshwater to discharge into the sea through the seepage window. A constant in time infiltration rate of 32 mm/year was applied over the entire surface boundary, except for few areas (dunes near the coastal boundary), which were subjected to a doubled infiltration rate of 64 mm/year.

A leakage from the lower confined aquifer was considered, imposing 121 point sources located in the western boundary of the aquifer bottom, each of  $2.0 \times 10^{-3} \text{ m}^3/\text{s}$  of freshwater flux, for a total recharge of  $241 \times 10^{-3} \text{ m}^3/\text{s}$  ( $7.6 \times 10^6 \text{ m}^3/\text{year}$ ).

Variable pumping rates at 953 clustered wells, with penetrations at two different depths of 30 and 45 m, were imposed with a maximum total extraction of  $50 \times 10^6 \text{ m}^3/\text{year}$ .

**First set of simulations.** A steady state simulation of the flow model was run, with the aquifer initially completely saturated at a uniform equivalent freshwater pressure head of zero throughout. The simulation takes into account leakage ( $7.6 \times 10^6 \text{ m}^3/\text{year}$ ), natural recharge ( $6 \times 10^6 \text{ m}^3/\text{year}$ ) and pumping at a rate of 37% of the maximum total extraction ( $18.50 \times 10^6 \text{ m}^3/\text{year}$ ). The hydraulic conductivity values were calibrated to best reproduce the “reference” piezometric field (1962).

Figure 2 compares the steady state simulated water table elevation above sea level (a.s.l.) with the values recorded at the observation wells in 1962, which was used as the starting point for the transient simulations

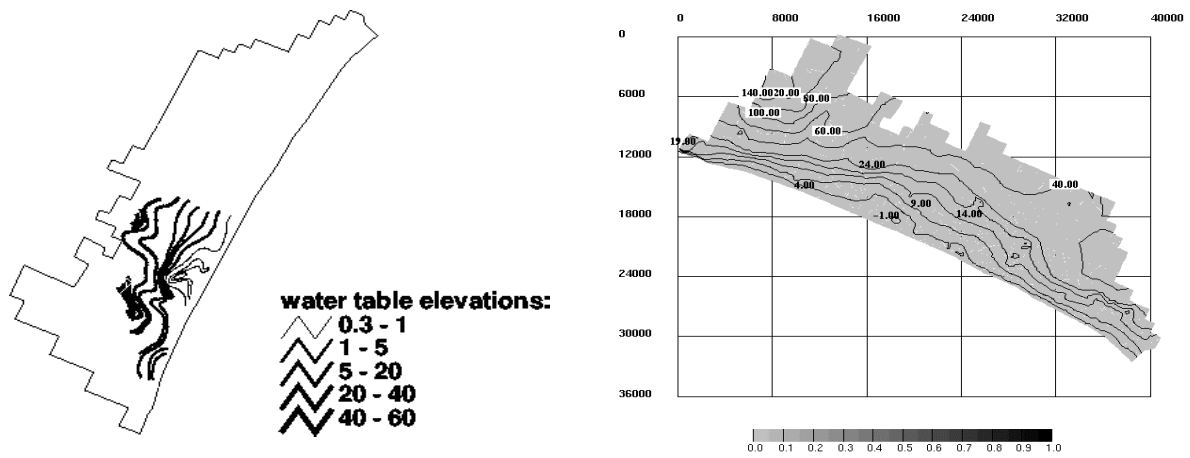


Figure 2. Comparison between field measured (left) and calculated (right) water table elevations (m a.s.l.) taking into account leakage, natural recharge, and weak pumping for the steady state flow simulation.

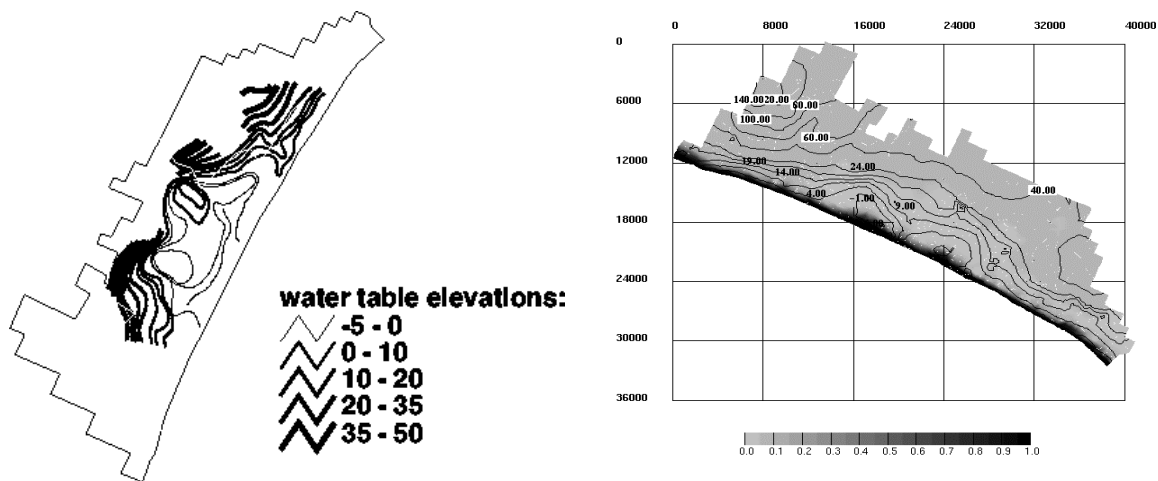


Figure 3. Comparison between field measured (left) and calculated (right) water table elevations (m a.s.l.) at 35 years (1996) for the transient coupled flow and transport simulation (scenario (a)). The concentration field is also shown in the right image.

described below. Although differences exist with field data, the correspondence is relatively good.

In the calibration process the parameters which most heavily influenced the behavior of the system were the imposed boundary conditions, namely the prescribed head along the river beds, the infiltration rate, and the saturated hydraulic conductivity. The adopted parameters were util-

ized for the subsequent transient flow and mass transport simulations.

**Second set of simulations.** A second set of simulations was run using the steady state conditions from the first set as initial conditions for the flow field. Initial conditions for the relative salt concentration were set assuming an ideal interface (not miscible) between salt- and freshwater according to the

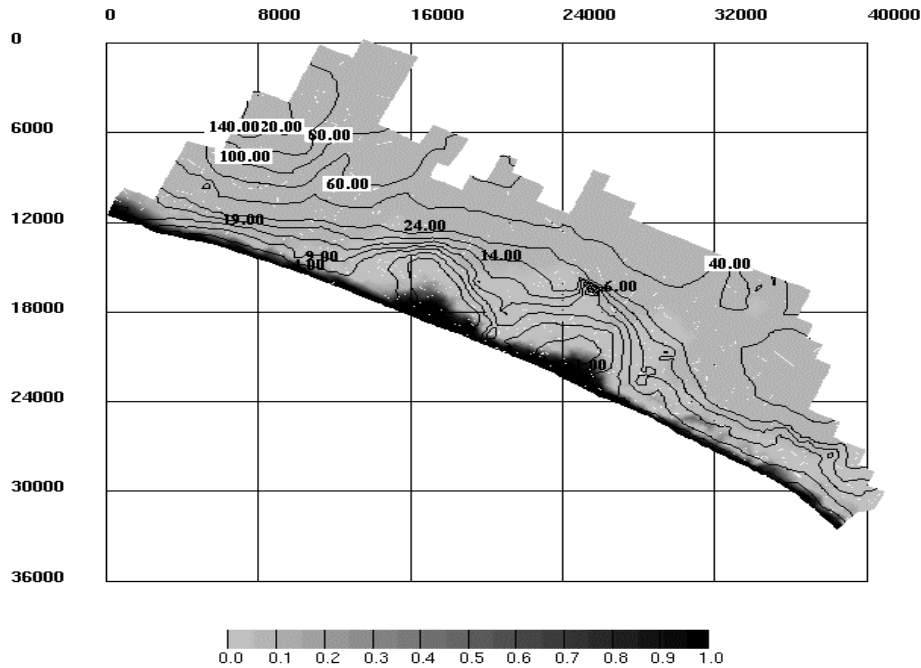


Figure 4. Calculated water table elevations (m a.s.l.) and saltwater concentrations at 35 years (1996) for the transient coupled flow and transport simulation (scenario (b)).

Ghyben-Herzberg approximation (Bear, 1979):  $h_s = h_0/\varepsilon$ , where  $h_s$  is the depth of a stationary interface below sea level and  $h_0$  is the phreatic level above sea level. That is we assume, at any distance from the sea, that the depth of the interface below the sea is 40 ( $=1/0.025$ ) times the height of the water table above it.

A period of 35 years was simulated. In this second set, pumping at variable rates was applied to the aquifer. Applying the maximum total exploitation rate for 35 years would have resulted in a severe water table lowering and at the end an almost complete drainage of the aquifer.

**Scenario (a).** Pumping rates linearly increasing from  $18.50$  to  $35 \times 10^6 \text{ m}^3/\text{year}$  during the entire simulation time. Figure 3 shows the water table drawdown at the end of the period and the saltwater concentration field along the water table surface for the same period. The pumping area is evident in the figure from the flow field. The depression cones, “artificially” separated by the river network, have a maximum depth of  $-6\text{m}$ ,

which is reasonably near to the observed field values. The results of the simulations show that water withdrawal from pumping has caused significant saltwater encroachment.

**Scenario (b).** Pumping rates linearly increasing from  $18.50$  to  $50 \times 10^6 \text{ m}^3/\text{year}$  during the entire simulation time. The pumping area is evident in Figure 4 both from the flow field and from the deflection of the saltwater front towards the two major upcoming zones. The depression cones have a maximum depth of  $-14 \text{ m}$ , which has been observed in the Korba plain during 1996.

**Scenario (c):** To analyze the impact of aquifer artificial replenishment, the same period of 35 years was also simulated considering an additional hypothetical recharge of  $1.3 \times 10^6 \text{ m}^3/\text{year}$  distributed in a few points belonging to the dune regions near the coast. Figure 5 shows that the saltwater concentration isolines for the run are significantly closer to the coastal boundary than in the previous cases, showing the induced effect of the freshwater discharge into the sea.

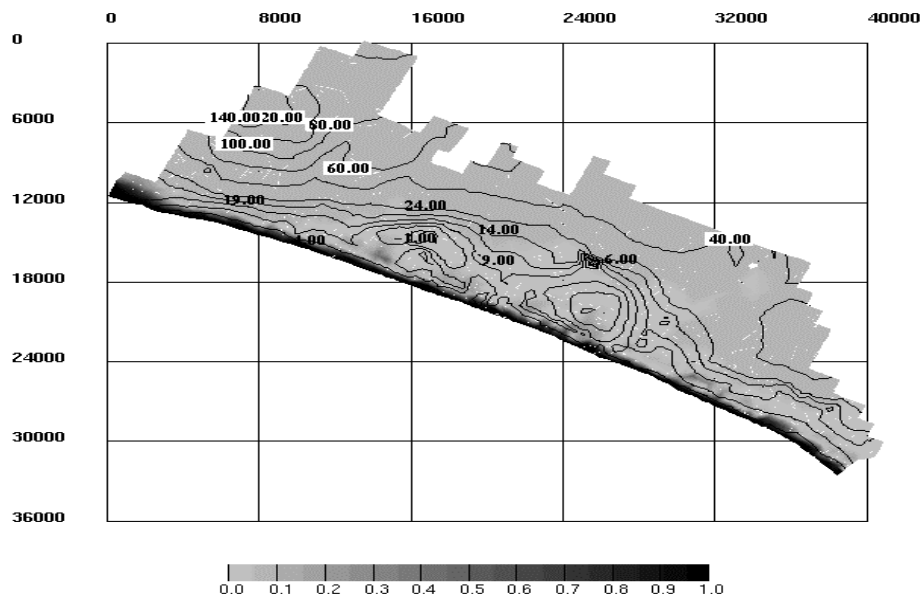


Figure 5. Calculated water table elevations (m a.s.l.) and saltwater concentrations at 35 years (1996) for the transient coupled flow and transport simulation (scenario (c)). Note the retreating saltwater front in comparison to the previous scenarios.

With regards to the coupled flow and transport simulation in both pumping and recharge conditions, the calculated equiconcentration lines did not agree well with the measured salinity contour lines shown in Figure 1, probably due to aforementioned lack of information about material and hydraulic parameters and to inadequate field data representation in space and time.

Two other simulations were run in order to investigate the influence of the sea seepage face window. A window depth of 30 m was used in the first run and a depth of 5 m in the second. The relative salinity field difference between the two cases for a transient simulation of 10 years with both infiltration and heavy pumping has a mean value of 0.0015 and a standard deviation of 0.011.

#### ACKNOWLEDGMENTS.

This work has been supported by the European Commission through grant number AVI-CT93-2-073 and by the Sardinia Regional Authorities.

#### BIBLIOGRAPHY

Bear, J. (1979). *Hydraulics of Groundwater*, McGraw-Hill, New York, NY.

Ennabli, M. (1977). *Etude sur modèle mathématique des aquifères du Nord-Est de la Tunisie*, PhD thesis, CIG-Ecoles des Mines, Paris, France.

Frind, E.O. (1982). Simulation of long-term transient density-dependent transport in groundwater, *Adv. Water Resour.*, 5, 73-88.

Gambolati, G., M. Putti, and C. Paniconi, (1998). Three-dimensional model of coupled density-dependent flow and miscible salt transport in groundwater, in *Seawater Intrusion in Coastal Aquifers: Concepts, Methods, and Practices*, A.H.-D.Cheng et al., eds. Kluwer Academic, Dordrecht, Holland. (To appear).

Khlaifi, I., G. Lecca, A. Giacomelli, J. Tarhouni, and C. Paniconi, GIS data analysis and application of a 3-D variably saturated seawater intrusion model to the Korba aquifer (Abstract). Presented at the Chapman Conference on "Application of GIS, Remote Sensing, Geostatistics, and Solute Transport Modeling to the Assessment of Non-Point Source Pollutants in

the Vadose Zone”, October 19-24, 1997, Riverside, California, CA.

Lecca, G., I. Khlaifi, J. Tarhouni and C. Paniconi (1998), Modeling seawater intrusion in the Korba aquifer (Tunisia). To appear in Proceedings of the XII International Conference on Computational Methods in Water Resources, June 15-19, 1998, Crete, Greece.

Putti, M. and C. Paniconi, (1995). Picard and Newton linearization for the coupled model of saltwater intrusion in aquifers, *Adv. Water Resources*, 18, 159-170.